A water coverage extraction approach to track inundation in the Saskatchewan River Delta, Canada

Article *in* International Journal of Remote Sensing · February 2015

DOI: 10.1080/01431161.2014.1001084

CITATIONS
11

READS
214

5 authors, including:

Zhanay Sagintayev
Nazarbayev University
37 PUBLICATIONS **134** CITATIONS

SEE PROFILE

Anton Sizo
Saskatchewan Research Council
9 PUBLICATIONS **48** CITATIONS

SEE PROFILE

Tim Jardine
University of Saskatchewan
97 PUBLICATIONS **2,317** CITATIONS

SEE PROFILE

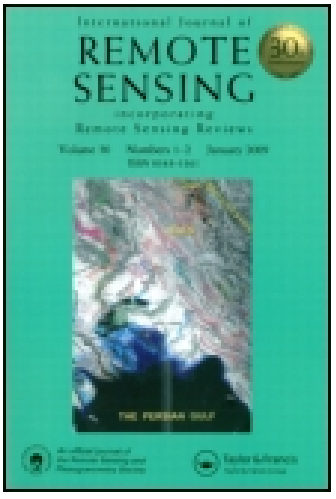

International Journal of Remote Sensing

Publication details, including instructions for authors and subscription information:
http://www.tandfonline.com/loi/tres20

A water coverage extraction approach to track inundation in the Saskatchewan River Delta, Canada

Jay Sagin[a], Anton Sizo[b], Howard Wheater[a], Timothy D. Jardine[c] & Karl-Erich Lindenschmidt[a]

[a] Global Institute for Water Security, School of Environment and Sustainability, University of Saskatchewan, Saskatoon, Canada

[b] Department of Geography and Planning, University of Saskatchewan, Saskatoon, Canada

[c] Toxicology Centre, School of Environment and Sustainability, University of Saskatchewan, Saskatoon, Canada

Published online: 09 Feb 2015.

To cite this article: Jay Sagin, Anton Sizo, Howard Wheater, Timothy D. Jardine & Karl-Erich Lindenschmidt (2015) A water coverage extraction approach to track inundation in the Saskatchewan River Delta, Canada, International Journal of Remote Sensing, 36:3, 764-781, DOI: 10.1080/01431161.2014.1001084

To link to this article: http://dx.doi.org/10.1080/01431161.2014.1001084

International Journal of Remote Sensing, 2015
Vol. 36, No. 3, 764–781, http://dx.doi.org/10.1080/01431161.2014.1001084

Taylor & Francis
Taylor & Francis Group

A water coverage extraction approach to track inundation in the Saskatchewan River Delta, Canada

Jay Sagin[a], Anton Sizo[b], Howard Wheater[a], Timothy D. Jardine[c], and Karl-Erich Lindenschmidt[a]*

[a]*Global Institute for Water Security, School of Environment and Sustainability, University of Saskatchewan, Saskatoon, Canada;* [b]*Department of Geography and Planning, University of Saskatchewan, Saskatoon, Canada;* [c]*Toxicology Centre, School of Environment and Sustainability, University of Saskatchewan, Saskatoon, Canada*

(*Received 2 August 2014; accepted 29 November 2014*)

Tracking surface water coverage changes is a complicated task for many regions of the world. It is, however, essential to monitor the associated biological changes and bioproductivity. We present a methodology to track contemporary water coverage changes using optical remote sensing and use it to estimate historical summer water coverage in a large river delta. We used a geographical information system automated routine, based on the modified normalized difference water index, to extract the surface water coverage area (SWCA) from optical satellite data sets using the surface water extraction coverage area tool (SWECAT). It was applied to measure SWCA during drought and flood peaks in the Saskatchewan River Delta in Canada, from Landsat, SPOT and RapidEye images. Landsat results compared favourably with Canadian National Hydro Network (CNHN) GeoBase data, with deviations between SWCA classifications and the base CNHN GeoBase shapefile of ~2%. Difference levels between the extracted SWCA layer from Landsat and the higher resolution commercial satellites (SPOT and RapidEye) were also less than 2%. SWCA was tightly linked to discharge and level measurements from in-channel gauges ($r^2 > 0.70$). Using the SWCA *versus* discharge relationship for the gauge with the longest record, we show that peak summer SWCA has declined by half over the last century, from 13% of our study area to 6%, with likely implications for fish and wildlife production.

Introduction

Tracking surface water coverage change is a vital task for water management (flood and droughts) and monitoring biological changes. This task is both challenging and important for large, remote areas subject to inundation such as river deltas. Large inland deltas in boreal regions have been long-standing hubs for fish and fur production (Townsend 1975; van de Wolfshaar et al. 2011). Profound hydrological changes owing to upstream impoundments have altered the flood characteristics of many of these deltas (Prowse et al. 2002; DUC 2011). One such delta, the Saskatchewan River Delta (SRD) (Figure 1), covers approximately 10,000 km^2 in the boreal plains ecoregion of Canada. Despite recent large-scale flood events (2005 and 2013) that have led to community evacuations (Smith and Pérez-Arlucea 2008), there has been a general declining trend in river discharge over the past half-century (DUC 2011). Understanding links between in-channel discharge,

*Corresponding author. Email: karl-erich.lindenschmidt@usask.ca

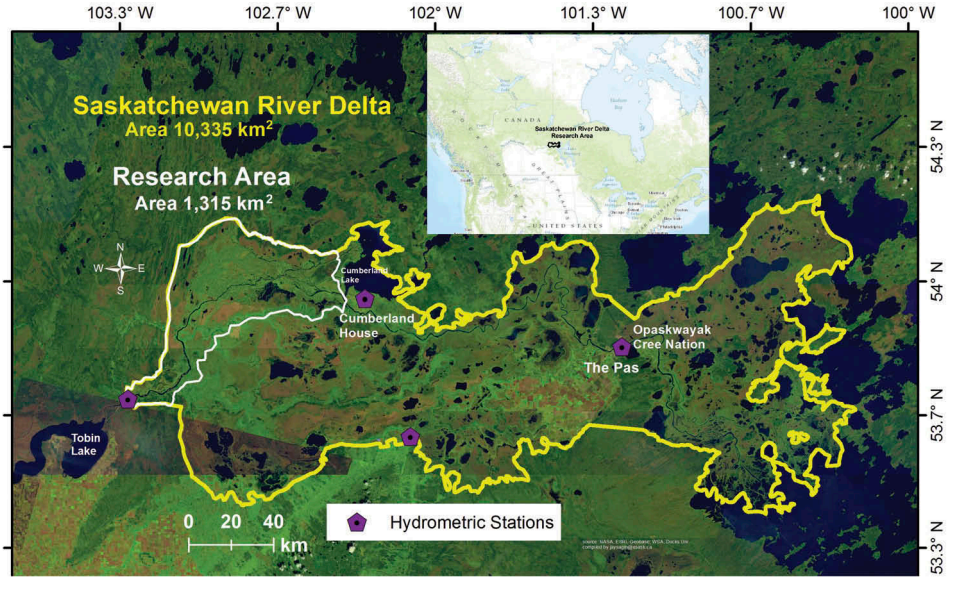

Figure 1. The study area in the Saskatchewan River Delta (SRD), Canada. Hydrometric station locations are indicated by purple pentagons (Saskatchewan River below Tobin Lake, station ID # 05KD003; Cumberland Lake, station ID # 05KH002; The Pas station ID # 05KJ001).

water level, and inundated area is therefore vital to determining the past, current, and future distribution of aquatic habitats as well as to the management of flood and drought risks.

Remote-sensing (RS) data sets are widely used for wetland inundation studies and are particularly useful for capturing hydrological processes occurring on large spatial scales (Hess and Melack 2003; Frohn et al. 2009; DUC 2011; Fantin-Cruz et al. 2011; van de Wolfshaar et al. 2011; Frohn et al. 2012; Sagintayev et al. 2012; Ward et al. 2013). While there are many successful cases of RS applications for floods and droughts, there are still many opportunities for improvement (Kuenzer et al. 2014). Some of the issues connected to these applications are the availability of satellite image data, issues of detecting water under vegetation canopies, cloud and smoke, application and selection of data with reasonable spatial resolution, and choices between free publicly available data and expensive commercial data. Freely available RS data typically have lower spatial resolution compared to commercial products. Most data with coarse spatial resolution, such as Moderate Resolution Imaging Spectroradiometer (MODIS) b1 and b2 with 250 m resolution, are available for free public use. Higher resolution data, up to 2–5 m (e.g. SPOT and RapidEye), are only commercially available and often out of the realm of many research budgets. Landsat is one of the exceptions, with a spatial resolution of 30 m and a 16-day revisit interval. Data stemming back to 1973 are freely available and acquisitions are continuing due to the recent launch of Landsat-8, Landsat Data Continuity Mission (launched in February 2013).

Selection of input data with reasonable spatial resolution that is appropriate to the size of the research area and the time constraints of research programmes are both critical considerations when choosing RS data sets. What methodology can be applied or is required to study changes in surface water coverage?

In this article, a methodology for extracting surface water coverage area (SWCA) is presented. We introduce an automated routine and toolset, designed in the geographical information system (GIS) environment, which reliably provides SWCA extracted from different satellite data sets. We tested our specialized GIS-based toolset by extracting a series of images from multiple satellites (Landsat, SPOT, and RapidEye). Water coverage layers from SPOT and RapidEye were used to compare with Landsat water extracted layers. The toolkit was applied to the SRD and relationships between inundated area and in-channel gauge measurements were examined, thus allowing hindcasting of past flood conditions in this important and vulnerable ecosystem.

Earth observation satellites with visible/infrared sensors from satellites such as Landsat, SPOT, IKONOS, RapidEye, ASTER, MODIS, NOAA AVHRR, IRS-1B LISS-II, and the radar systems JERS-1, ERS-1, and RadarSat have been used widely for surface monitoring, especially coverage tracking of large areas (Li et al. 2001; Ozesmi and Bauer 2002; Lee and Anagnostou 2004; Töyrä and Pietroniro 2005; Fournier et al. 2007; Lacaux et al. 2007; Sultan et al. 2008; Milewski et al. 2009; Sagintayev et al. 2012). The water coverage extraction methods can be divided into four types (Ozesmi and Bauer 2002; Feyisa et al. 2014): (i) thematic methods, including unsupervised classifications or clustering using principal component analysis (Wagner et al. 2003; Lira 2006; Jensen 2007); (ii) supervised classification, including the popular maximum likelihood method; (iii) variations of satellite-derived indices, including single-band thresholding (Jain et al. 2005), two-band spectral indices (Jain et al. 2006), such as the normalized difference water index (NDWI) (McFeeters 1996), the normalized difference moisture index (Wilson and Sader 2002), the modified normalized difference water index (mNDWI) (Xu 2006; Ji, Zhang, and Wylie 2009), the water index (Ouma and Tateishi 2006), normalized difference vegetation index (NDVI) (Gao 1996), and the automated water extraction index (AWEI) (Feyisa et al. 2014); and (iv) a combination of various methods, fuzzy classification, subpixel classification, spectral mixture analysis, hybrid or rule-based methods (Ozesmi and Bauer 2002; Jensen 2007; Rokni et al. 2014).

Methodology

Method testing site description

The study area is the SRD at the lower end of the Saskatchewan River Basin (SRB) in Canada. The entire delta spans approximately 10,000 km^2 (yellow polygon), so a subsection (white polygon) covering 1315 km^2 was selected as a test site (Figure 1). The hydrometric station locations are shown by purple pentagons (Figure 1). Some tracking of vegetation changes has been carried out on a small area of the delta (Baschuk, Ervin, et al. 2012). Some studies covering the entire SRB emphasize land use and water quality in the basin (SRBPartners 2008). Field work in the region is complicated by the remote location and the large areas of shallow water, bogs, fens, swamps, and marshes, such as the Summerberry Marsh (DUC 2011). The SRD is a low-lying and low-slope area with substantial wet and dry fluctuations from spring to summer (SRBPartners 2008). It is an important bird breeding area consisting of a complex series of abandoned and active river channels, lakes, and wetlands (Adams, Slingerland, and Smith 2004; Baschuk, Koper, et al. 2012). Moreover, the SRD water regime is a culmination of runoff water diversions and extractions and dam regulations, all occurring upstream in the SRB (Schindler and Donahue 2006). Annual discharge has been reduced by approximately 30% since the beginning of the last century due in part to both the Gardiner and E.B. Campbell dams withholding flow (DUC 2011). At the

same time, floods inundate large areas of the delta, impacting local residents. The SRD is therefore prone to both flood and drought. Recent extreme floods occurred in 2005, 2011, and 2013, while 2001 and 2002 were extreme drought years (Schindler and Donahue 2006; Smith et al. 2009; DUC 2011). These dynamics make it critical to understand how surface water coverage varies with in-channel flow as measured by gauges.

Satellite and gauge data

Water-related GIS data sets such as the flow network and water coverage of the research area were acquired from Canadian National Hydro Network (CNHN) data sets (http://www.geobase.ca). Landsat data were obtained from the United States Geological Survey Earth Resources Observation and Science Center's Global Visualization Viewer (http://glovis.usgs.gov/). The SPOT data sets were acquired from the Alberta Terrestrial Imaging Center, and the RapidEye data sets were purchased from BlackBridge Geomatics. Landsat consistently collects data by rows and paths that are made available using a well-developed processing methodology. Only data sets without cloud coverage were selected for this study and image calibrations with atmospheric corrections were also used. The same consistent UTM projections were applied to all data sets, including SPOT, RapidEye, Landsat, and Geobase. Hydrometric gauge data were acquired from the Water Survey of Canada, Environment Canada (http://www.ec.gc.ca/rhc-wsc/).

Methods review: mNDWI

From the various surveyed methods for extracting SWCA, normalized spectral indices, manual translation, and parametric classification of images are the most widely used (Gao 1996; Xu 2006; Lacaux et al. 2007; Ji, Zhang, and Wylie 2009). In comparison to other methods, the use of spectral indices has many advantages; this method relies primarily on the transformation of numerical values, which allows a decrease in background effects and reduced data dimensionality to provide a level of standardization for comparative purposes, and enhance the required signal for specific land-cover and land-use areas (Reed et al. 1994). Thus, normalized indices increase the separation ability of information extracted from RS data. Due to spectral differences among diverse land-cover and land-use areas, surface areas can be calculated from different combinations of remotely sensed image bands depending on the type of surface analysed, for example water, vegetation, or urban areas (As-Syakur et al. 2012).

The current research adapted the approach of normalized spectral difference indices for the identification of water areas. Here, the NDWI in the form of the mNDWI was used for the delineation of open surface water areas within the studied region:

$$\mathrm{mNDWI} = \frac{B_{\mathrm{green}} - B_{\mathrm{SWIR(NIR)}}}{B_{\mathrm{green}} + B_{\mathrm{SWIR(NIR)}}}, \tag{1}$$

where B_{green} and $B_{\mathrm{SWIR(NIR)}}$ are sensor spectral parameters. B_{green} is the green band (wavelength 0.5–0.6 μm). B_{NIR} is the near infrared band (wavelength 0.7–0.9 μm) with small variations between Landsat MMS, SPOT2 HRV, and RapidEye JSS56 B_{NIR} sensors. B_{SWIR} is the short-wave infrared band (wavelength 1.55–1.75 μm) with small variations between Landsat TM, SPOT4 HRVIR, and SPOT5 HRG B_{SWIR} sensors.

The mNDWI depends on the proportion of water subpixels to non-water subpixels (e.g. soil and/or vegetation). Applying a threshold can control the analysis output (Ji, Zhang, and Wylie 2009). Following Xu (2006), zero was set as the mNDWI threshold for open surface water areas. In addition to the water index threshold, the $B_{\mathrm{SWIR(NIR)}}$ thresholds were used for better open surface water area identification and delineation (Lacaux et al. 2007). The $B_{\mathrm{SWIR(NIR)}}$ thresholds were estimated for the satellite data sets using a visual assessment of the preliminary identification results (Table 1). The following are the different mNDWI threshold pixel value limits of the $B_{\mathrm{SWIR(NIR)}}$ used for open surface water area identification and delineation: (a) Landsat MSS (NIR) – 30; (b) Landsat TM (SWIR) – 35; (c) Landsat ETM + (SWIR) – 35; (d) SPOT2 HRV (NIR) – 40; (e) SPOT4 HRVIR (SWIR) – 40; (f) SPOT5 HRG (SWIR) – 60; and (g) RapidEye JSS56 (NIR) – 2500 (Table 1). RapidEye's threshold is higher because it has a higher radiometric resolution (16 bit data) compared to Landsat and SPOT (8 bit data). By using these thresholds, the SWCAs were extracted.

The general spatial resolution rule states that for the successful identification of the object of interest there is a need for at least four spatial observations – pixels, in the case of RS raster data (Cowen et al. 1995; Jensen 2007). For example, the identification of a water object with a 60 m diameter would require four pixels with at least 30 m × 30 m spatial resolution. Therefore, the identified open surface areas were filtered: the objects less than or equal to the area of three pixels were removed to avoid misinterpretation. After filtering, the identified open surface areas that intersected the study region were extracted as a final result.

A toolset for surface water coverage extraction

A GIS-based toolset was designed for the surface water coverage extraction from different satellite data sets. We prepared the mNDWI tool using Environmental Sciences Research Institute (Esri) ArcGIS visual programming capabilities to extract the SWCA. Referring to Figure 2 for the conceptual scheme of the mNDWI tool, the logic of the tool's algorithm includes (i) mathematical calculations, i.e. mNDWI calculation with the input of green and SWIR (NIR) band values (Equation (1)) and the application of mNDWI, SWIR(NIR), and data filtration 3 pixels thresholds; (ii) Boolean operation, i.e. AND between mNDWI and SWIR(NIR) layers after respective thresholds application; and (iii) the overlay operation, i.e. Intersect, which extracts the final SWCA within the study area. The use of the mNDWI approach and Esri ArcGIS visual programming capabilities provides users with reliable output and calculation flexibility. It is a time-efficient method and can be embedded into one's GIS data flow.

We applied the new toolset to determine the SWCA and to track hydrological changes for flood years in the SRD. The SWCA extracted from Landsat were then compared with the SWCA from CNHN, SPOT, and RapidEye on dates as close as possible to the Landsat acquisitions and for as broad a range as possible of surface coverage.

To compare the SWCA with the in-channel and lake gauge data, spring and summer peaks were analysed separately because they represented local snowmelt runoff and riverine flow originating in the Rocky Mountains, respectively. We examined the shape and strength of relationships between the SWCA and discharge for two gauges (05KD003, Saskatchewan River below Tobin Lake, and 05KJ001, Saskatchewan River at The Pas) and between the SWCA and level for a third gauge (05KH002 Cumberland Lake). All data from 1985 to 2012 were combined to include the range of flow conditions

Table 1. Dates of image acquisitions: level type (rise, peak, recession); sensor type; threshold type (SWIR or NIR) number; discharge (discharge gauge station ID # 05KD003, Saskatchewan River below Tobin Lake); water level (from 264 m as a zero point, hydrometric water stage station ID # 05KH002, Cumberland Lake); spring SWCA; summer SWCA.

Date	Level	Sensor	Threshold	Discharge ($m^3 s^{-1}$)	Water level (m)	Spring SWCA (km^2)	Summer SWCA (km^2)	Date	Level	Sensor	Threshold	Discharge ($m^3 s^{-1}$)	Water level (m)	Spring SWCA (km^2)	Summer SWCA (km^2)
14 May 2011	Rise	TM5	35	1310	2.48	233		3.06.1995	Rise	TM5	35	308			54
30 May 2011	Rise	TM5	35	1370	2.72	159		5.07.1995	Rise	TM5	35	963			99
7 June 2011	Rise	ETM7	35	1760	2.81	176		14 July 1995	Peak			1580			
27 June 2011	Peak			3270	3.59			6 August 1995	Recess	TM5	35	555			68
9 July 2011	Recess	ETM7	35	1730	4.43		254	7 August 1995	Recess	TM5	35	350			63
17 July 2011	Recess	TM5	35	1060	4.05		191	8 May 2012	Rise	ETM7	35	600	1.62	83	
29 July 2011	Recess	RapidEye	2500	1050	3.51		178	24 May 2012	Rise	ETM7	35	557	1.75	93	
2 August 2011	Recess	TM5	35	978	3.33		146	30 June 2012	Peak			1258	2.27		
10 August 2011	Recess	ETM7	35	855	3		123	4 July 2005	Peak			1243	2.3		
19 September 2011	Recess	TM5	35	425	2.59		88	9 July 2012	Recess	RapidEye	2500	1217	2.46		106
21 October 2011	Recess	TM5	35	435	2.49		74	11 July 2012	Recess	ETM7	35	1198	2.47		105
19 April 2005	Rise	ETM7	35	992	2.63	227		13 September 2012	Recess	ETM7	35	411	1.54		87
5 May 2005	Rise	ETM7	35	434	2.1	112		29 September 2012	Recess	ETM7	35	229	1.2		87
8 June 2005	Rise	SPOT4	60	1110	1.74		151	23 April 1985	Peak	TM5	35	1100			
22 June 2005	Rise	ETM7	35	2470	1.74		183	9 July 1985	Recess	TM5	35	393			73

(*Continued*)

Table 1. (*Continued*).

Date	Level	Sensor	Threshold	Discharge ($m^3 s^{-1}$)	Water level (m)	Spring SWCA (km^2)	Summer SWCA (km^2)	Date	Level	Sensor	Threshold	Discharge ($m^3 s^{-1}$)	Water level (m)	Spring SWCA (km^2)	Summer SWCA (km^2)
23 June 2005	Peak			2870	2.35			11 September 1985	Recess	TM5	35	180			48
30 June 2005	Peak			2550	3.17			14 July 2000	Peak			737			
8 July 2005	Recess	SPOT4	60	1810	3.67		289	27 August 2000	Recess	ETM7	35	328	1.27		64
8 July 2005	Recess	ETM7	35	1810	3.67		292	8 August 2001	Rise	ETM7	35	228	1.27	71	
31 July 2005	Recess	SPOT2	40	488	2.51		101	2 May 2001	Rise	TM5	35	319	1.25	58	
1 August 2005	Recess	TM5	35	717	2.51		94	3 June 2001	Rise	TM5	35	242	0.62		49
2 September 2005	Recess	TM5	35	778	1.8		98	1 August 2001	Peak		35	516	0.9		
26 September 2005	Recess	ETM7	35	1030	2.61		179	6 August 2001	Recess	TM5	35	327	1.07		56
12 October 2005	Recess	ETM7	35	648	2.42		178	15 September 2001	Recess	ETM7	35	333	0.49		53
5 June 1990	Rise	TM5	35	919		172		1 October 2001	Recess	ETM7	35	162	0.41		44
8 July 1990	Peak			2100				9 October 2001	Recess	TM5	35	179	0.43		45

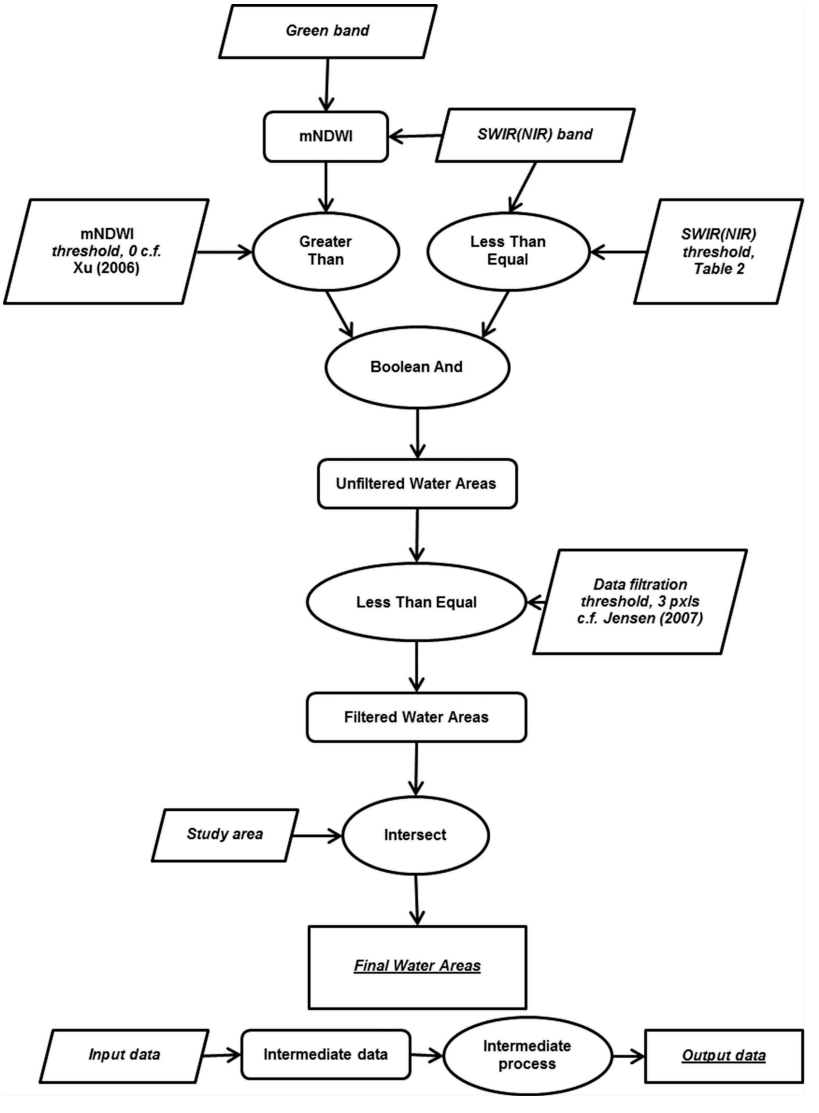

Figure 2. Conceptual diagram illustrating the application of the mNDWI tool developed using ArcGIS visual programming capabilities to extract SWCA from Landsat TM, SPOT, and RapidEye satellite data sets.

across drought, average flow, and flood years (Table 1). Cumberland Lake water level was available only from 2000 onwards, and the lake zero point is 264 m above sea level.

To examine how the SWCA has changed over the time period for which records were available, we used the regression relationship developed between the SWCA and discharge for the gauge at The Pas. We applied the corresponding regression equation to the entire record (1913–2012) and estimated daily SWCA for the summer months (June to September) because biological activity in flooded areas are most likely to peak when temperatures are warm and the photoperiod is long (Winemiller 2004). We then

determined the maximum and minimum summer SWCA for each recorded year and determined change over time using linear regression.

Results

The applied methodology with the toolset allowed identification of the SWCA during drought and flood periods. The smallest SWCA of 56 km^2 in our image set occurred on 6 August 2001, a time period classified as drought conditions (Landsat TM, Figure 3(*a*)). An example of average SWCA conditions of 89 km^2 occurred on 13 September 1990 (Landsat TM, Figure 3(*b*)). The next SWCA level, 106 km^2, was on 9 July 2012 (RapidEye, Figure 3(*c*)). The following SWCA of 151 km^2 was captured during the 2005 flooding on 8 June 2005 (SPOT-4, Figure 3(*d*)). A higher SWCA of 178 km^2 occurred on 29 July 2011 (RapidEye, Figure 3(*e*)). The maximum SWCA of 289 km^2 was observed during flooding on 8 July 2005 (SPOT-4, Figure 3(*f*)).

Verification and deviations: data sets comparison

The SWCA extracted from Landsat were compared with SWCA from CNHN, SPOT, and RapidEye. The CNHN metadata (http://www.geobase.ca) provided validation data for the layer covering the research area for the following dates: 11 September 2002, 15 September 2001, and 24 July 1990, and for the years 1988, 1985, 1979, and 1968 (no day or month is

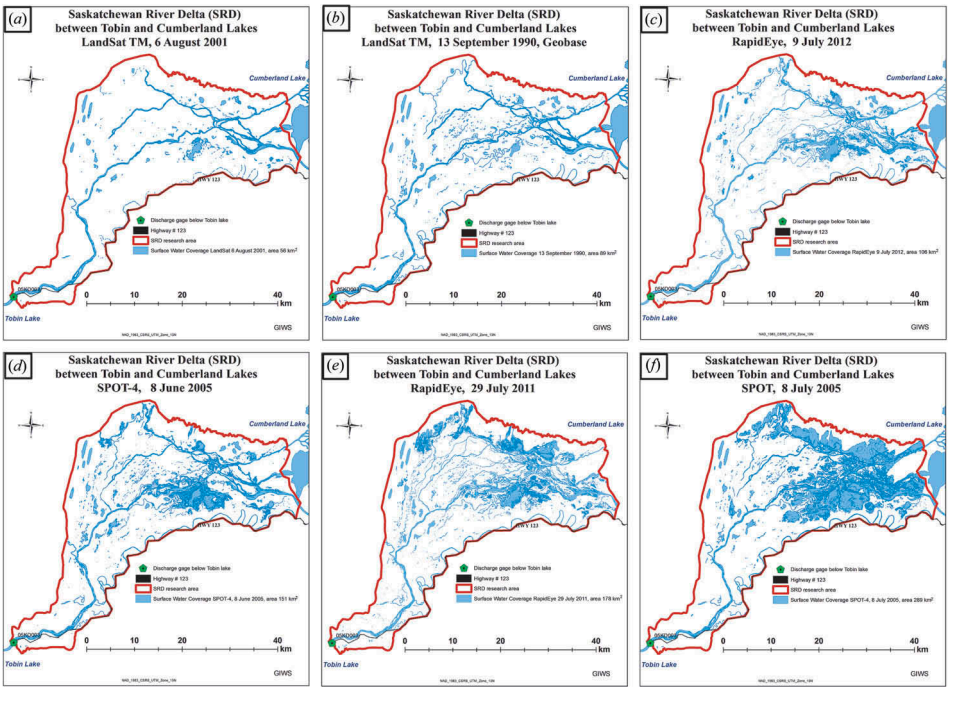

Figure 3. Examples of the extracted SRD SWCA for different times and satellite images: (*a*) Landsat TM, 6 August 2001 – SWCA = 56 km^2; (*b*) Landsat TM August 1990 – SWCA = 89 km^2; (*c*) RapidEye, 9 July 2012 – SWCA = 106 km^2; (*d*) SPOT-4, 8 June 2005 – SWCA = 151 km^2; (*e*) RapidEye, 29 July 2011 – SWCA = 178 km^2; and (*f*) SPOT-4, 8 July 2005 – SWCA = 289 km^2.

provided for these years). The CNHN metadata does not show the exact Landsat date, and obtaining more detailed information from the CNHN Geobase is not possible. According to the Geobase support technicians, the layers were prepared by using a combination of field data collection and different Landsat images acquired under average flow conditions, without droughts or flooding. Based on the available data from CNHN, we assumed that this coverage occurred on dates close to 11–15 September, typical of average flow conditions. The CNHN layer reports SWCA of 89 km^2; this value was used as a base for our SWCA comparison and verification for different years on dates near 11–15 September.

While many Landsat images were cloud-covered and thus excluded from the SWCA analysis, sufficient images were available to compare to the CNHN (Table 1) and yielded reasonable comparisons to CNHN-derived SWCA. Using the closest date to the CNHN date range, the following % differences were observed:

(*date; CNHN SWCA km^2; Landsat SWCA km^2; % difference*)

- 11 September 1985 48 89 –46%
- 9 September 1995 63 89 –29%
- 15 September 2001 53 89 –40%
- 2 September 2005 98 89 10%
- 19 September 2011 88 89 –1%
- 13 September 2012 87 89 –2%

The next verification level for Landsat-derived SWCA was a comparison to estimates obtained from SPOT and RapidEye during flood conditions (Table 1). Three pairs of images on comparable dates showed good agreement. The RapidEye (29 July 2011, discharge 1050 m^3 s^{-1}) and Landsat (17 July 2011, discharge 1060 m^3 s^{-1}) comparison shows 178/191 = 7 % difference, likely stemming from the two data sets being acquired on different days with slightly different discharge levels. The SPOT (8 June 2005, discharge 1110 m^3 s^{-1}) and Landsat (22 June 2005, discharge 2470 m^3 s^{-1}) comparison also shows a difference of 7% (151/183) despite the large differences in flow conditions and the 2-week interval between acquisition dates. The SPOT and Landsat images captured on the same day (8 July 2005, discharge 1810 m^{-3} s^{-1}) exhibited a difference of 289/292 = 1%. The explanation of the small difference in SWCA, even though there is high difference in discharge values, is related to the topography and geology of the SRD. The SRD is very flat with an average slope of 0.0001 (10 m elevation difference for a distance of 100 km). The study area is underlain by a shallow layer of limestone (Interlake Formation) of Ordovician and Silurian age resting upon Precambrian rocks of the Canadian Shield. Clay-rich glacial till is the dominant feature of the surficial geology (Morozova and Smith 2000). The SRD has a mixture of bog deposits, sand, silt, and clay with low permeability (PFRA 1977). During high river discharges, water moves mostly along the well-developed delta stream channels over the low-permeability deposits to Cumberland Lake.

Hydrometric stations and surface water coverage

There was good agreement between hydrometric gauge data and the SWCA derived from Landsat, SPOT, and RapidEye. Seasonal changes during two flooding years, 2005 and 2011, show how the SWCA varies over the course of the ice-free season (Figures 4 and 5), and image mosaics juxtaposed on the discharge and level hydrographs indicate synchrony. Major flood peaks occurring in late June and early July in both years and a minor peak in

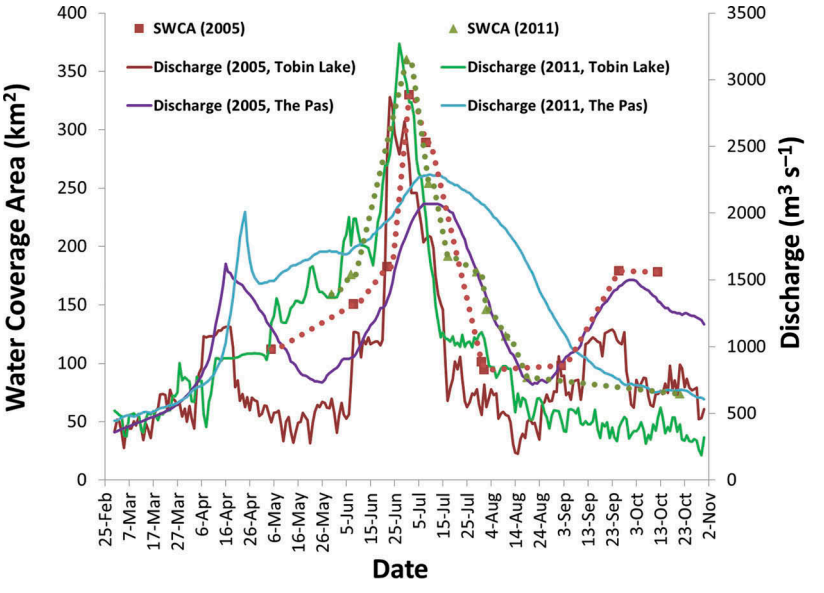

Figure 4. Time series of SWCA and discharge (station ID # 05KD003, Saskatchewan River below Tobin Lake; station ID # 05KJ001, Saskatchewan River at The Pas) for the 2005 and 2011 flood years. The hatched line corresponds to a 5-day moving average for SWCA.

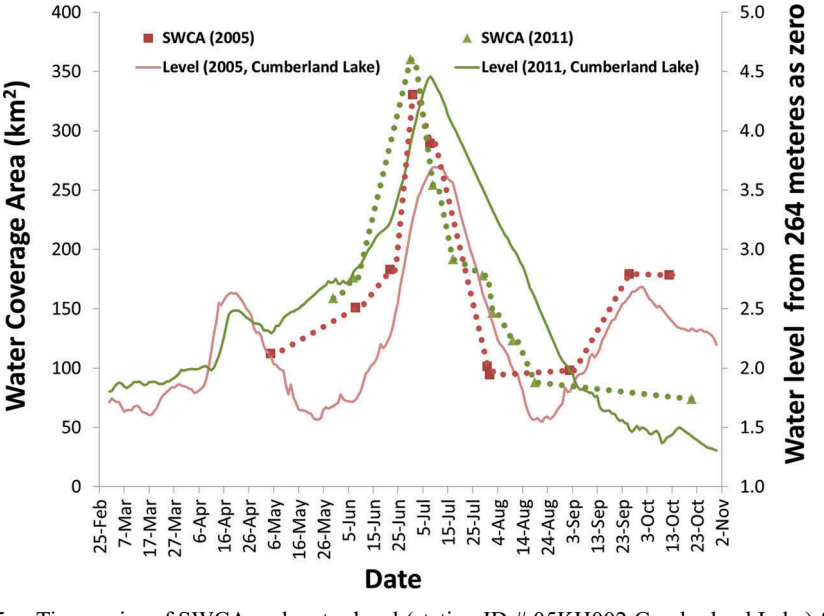

Figure 5. Time series of SWCA and water level (station ID # 05KH002 Cumberland Lake) for the 2005 and 2011 flood years.

fall 2005 were also captured by the SWCA method. There was a minor time lag between the discharge recorded at the most upstream gauge (Saskatchewan River below Tobin Lake) and the estimated SWCA, while the opposite was the case for the downstream gauges (Cumberland Lake and The Pas), consistent with their positions (Figure 1).

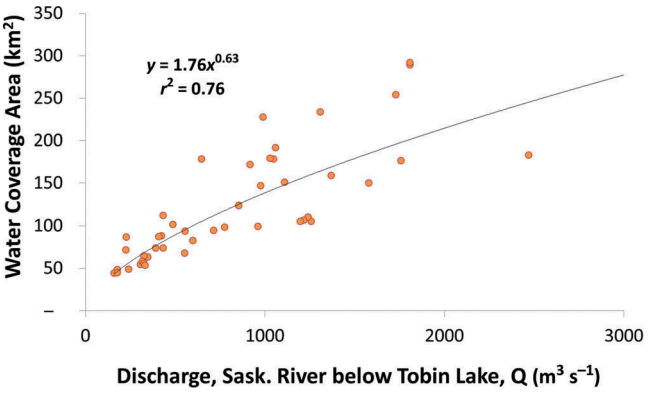

Figure 6. Relationship between extracted SWCA and discharge (station ID # 05KD003, the Saskatchewan River below Tobin Lake). The best fit power function is $y = 1.76x^{0.63}$ ($r^2 = 0.76$).

SWCA increased according to a power function of river discharge below Tobin Lake ($y = 1.76x^{0.63}$, $r^2 = 0.76$, Figure 6), while exponential functions best described the relationship between SWCA and level at Cumberland Lake ($y = 39.9e^{0.49x}$, $r^2 = 0.71$, Figure 7) and between SWCA and discharge measured at The Pas ($y = 44.872e^{0.0007x}$, $r^2 = 0.72$, Figure 8).

Both maximum and minimum summer SWCA declined during the 100-year record at The Pas (Figure 9). This change was more pronounced for maximum area (slope = −0.91, $r^2 = 0.20$) than minimum area (slope = −0.18, $r^2 = 0.16$). On average, approximately 1 km^2 less area has flooded each year since the beginning of the instrument record. In 1913, an average summer flood covered approximately 168 km^2, or 13% of our study area, while current floods cover approximately 78 km^2, or 6% of the study area.

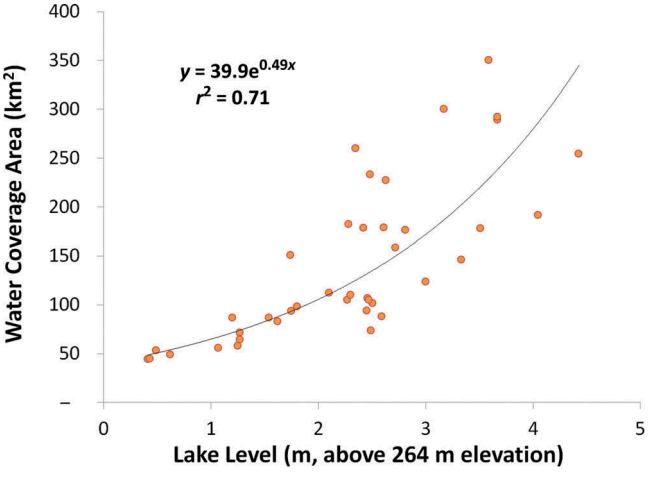

Figure 7. Relationship between extracted SWCA and water level from 264 m as zero point (station ID # 05KH002, Cumberland Lake). The best fit exponential function is $y = 39.9e^{0.49x}$ ($r^2 = 0.71$).

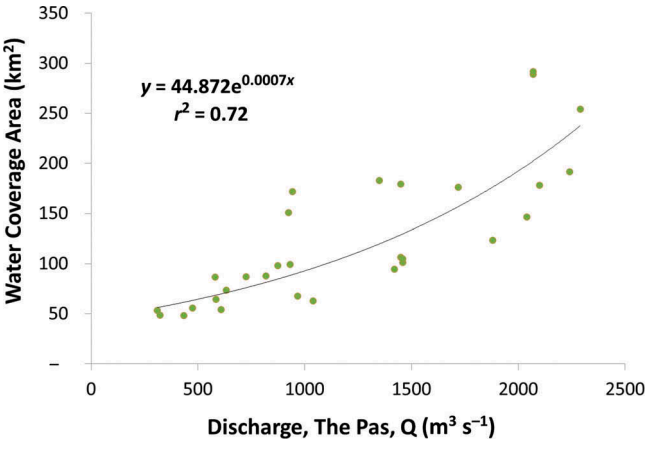

Figure 8. Relationship between extracted SWCA and discharge (station ID # 05KJ001, The Pas). The best fit power function is $y = 44.87e^{0.0007x}$ ($r^2 = 0.72$).

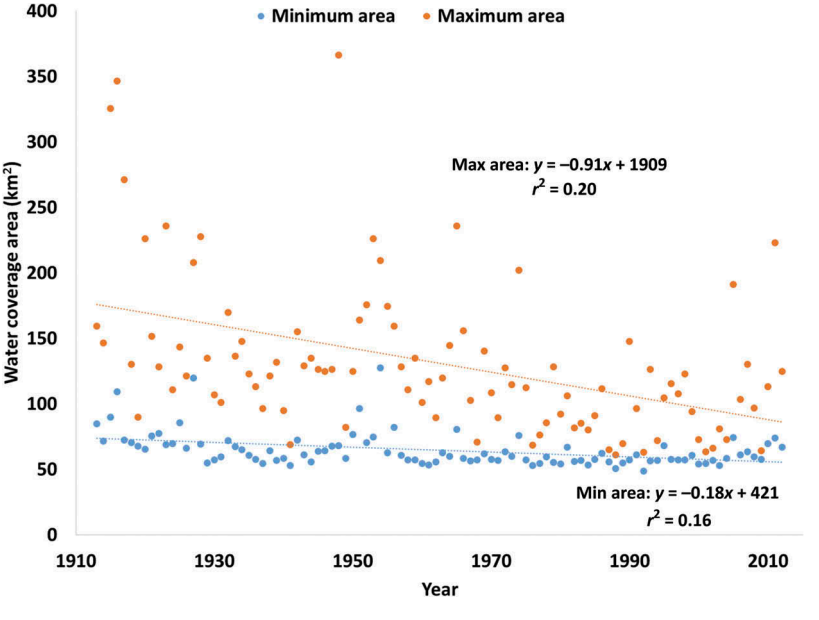

Figure 9. Estimated maximum and minimum summer SWCA over the past century, developed from the regression relationship in Figure 8 and applied to long-term gauge date from The Pas (1913–2012).

Discussion

The mNDWI methodology and toolset were applied to track SWCA for the wide-ranging hydrological regime of the SRD. The deviations between extracted SWCA layers compared to the base CNHN layer (range of differences = −10 to 46%) likely stem from variability introduced by flooding and droughts because the CNHN layer was developed

in the absence of these conditions. For example, an average year (2012) without droughts and floods yielded a result consistent with the CNHN (87/89 = 2%). Additional uncertainty arises from differences in acquisition dates between the CNHN water layers and the Landsat data set. Smaller deviations (<7%) observed between freely available Landsat imagery and commercial satellite data (SPOT and RapidEye) can also be attributed to offsets in acquisition dates as well as the difference in pixel sizes between products. SPOT (10 m spatial resolution) and RapidEye (5 m) both have higher spatial resolution than Landsat (30 m). However, for the purposes of RS applications in large river wetlands such as the SRD (total area ~10,000 km^2, smaller research area examined here = 1315 km^2), this deviation is acceptable. For similar tasks in large-scale areas, it may be rational to use Landsat images instead of expensive commercial satellite images such as those from SPOT and RapidEye (Ward et al. 2013), especially if budgets are constrained. The freely available and consistent Landsat, with a revisit interval of 16 days, is a viable option for these purposes while reserving more expensive, high-resolution data for fine-scale investigations (Baschuk, Ervin, et al. 2012). Landsat data have been one of the best sources for analysing land surface changes over the past 40 years (Dangermond 2013).

Our analyses show the timing and magnitude of river flow required to inundate large portions of the SRD. In 2011, flood water was released more gradually from Tobin Lake (flow controlled by E.B. Campbell dam) than in 2005, when water was held back from the end of April until early June before being released. Upon release, SWCA increases rapidly with comparable peaks in the two years despite the differences in release timing. It takes approximately two weeks to inundate the delta when the discharge exceeds more than 1500 m^{-3} s^{-1}, and infrastructure becomes threatened and levee deposition occurs at flows above 2500 m^{-3} s^{-1} (Smith and Pérez-Arlucea 2008). When the discharge is less than 1000 m^{-3} s^{-1}, water is conveyed mostly through stream channels and little inundation occurs, as evidenced by the small SWCA (<100 km^2) and its tight relationship with discharge at these low flows (Figures 6 and 8).

The strong correlation between in-stream gauge data and SWCA opens up possibilities for retrospective and prospective analyses of inundated area with implications for flood risk and biological production (Ward et al. 2013). For example, our hindcasting of SWCA shows that peak summer flooded area has gradually declined over the past century, likely due to capture and storage, followed by winter release, then hydro dams in the basin, combined with declining inflows (St. Jacques et al. 2010). Long-term declines in flows and floods are linked to reduced fish productivity in regulated basins (van de Wolfshaar et al. 2011) as the truncation of flood peaks limits the ability of plants and animal to capitalize on the 'flood-pulse advantage' (Bayley 1995). This reduction in flood pulsing is likely a factor involved in the notable declines in fish and wildlife production in the SRD (SRBPartners 2008).

The links between gauge data and inundated area may also enable future projections of floods associated with additional water resource development in the basin and climate change. The latter is predicted to reduce overall flows by 7% and alter seasonal timing, with summer declines of 15% and a shift towards earlier spring flooding in the SRB (Lapp, Sauchyn, and Toth 2009; Pomeroy et al. 2010; Shepherd, Gill, and Rood 2010; Sagintayev et al. 2013).

The main limitation of optical satellite sensors (Landsat, SPOT, and RapidEye) is fog and cloud coverage. In comparison with the optical satellites, the radar satellite signals are unimpeded by clouds and fog, and can collect data from almost any environment day or night. Radar imagery is available with resolutions as fine as 3 m. Radar satellites include RadarSat-2 (resolution: 3–100 m), Envisat (30–150 m), Cosmo-SlyMed (1–100 m), and TerraSAR-X (1–18 m), images that are all commercially available.

Conclusion

The methodology and the GIS mNDWI tool were developed and tested to trace surface water coverage and timing of inundation for the SRD using satellite images and a limited amount of gauge data. While SWCA correlates reasonably well with discharge and level data discharge, routing may improve the correlation for such a large and intricate stream network system. The KISTERS WISKI water resource management system may be well suited for such an application. Routing would (i) incorporate a lag-time between discharge from Tobin Lake and the downstream flooded surfaces and (ii) simulate accumulated volumes discharged from Tobin Lake, which affect the extent of flooding throughout the delta. Answers to these questions can be critical for flood forecasting, especially for the communities of Cumberland House in Saskatchewan and the Opaskwayak Cree Nation and The Pas in Manitoba.

The difference in the counts of water pixels between the extracted SWCA layer and the base CNHN layer is 2% for comparable data acquisitions. The difference between the extracted SWCA layer from Landsat and the higher resolution commercial satellites SPOT and RapidEye is also 2%. For large-scale studies, Landsat data may be sufficient to characterize surface water coverage, especially if constrained research budgets do not allow extensive expenditures for imagery acquisition. However, small-scale studies requiring fine spatial resolution may require imagery from commercial sensors such as SPOT and RapidEye.

This methodology was developed and tested on an area within the SRD; however, it may be applied to many other parts of the world with a similar hydrological setting on a large scale with a paucity of field data and availability of satellite images.

The optical satellite sensors, Landsat, SPOT, and RapidEye, have limitations during times of fog and cloud cover. In comparison to the optical satellites, radar is uninhibited by cloud and fog and can collect data both during the day and at night. A combination of optical and radar sensors may be a reasonable approach to improve temporal resolution and is a subject of future work.

Future studies should also be related to the analyses of SWCA, different discharge levels, and soil moisture. Testing other water indices, including the AWEI for flat areas, using imagery from available satellites sensors covering our area, is also planned. The AWEI has only been tested for mountainous areas using Landsat imagery, but it will be interesting to see how it performs for flat areas.

The small differences in SWCA when discharge values are high should be related to the topography and geology of the SRD. The SRD is a very flat area, and it is underlain by a shallow limestone layer, covered with surficial mixture of bog deposits, sand, silt, and clay with low permeability. The bog deposits during the dry seasons may work as a sponge and may store a large amount of water. During the wet period, soil is saturated and runoff is higher. The amount of water volume that the bogs store should also be investigated. This is a vulnerable area for flooding of residences and additional tools are required for better flood forecasting, especially for First Nation communities and areas around the town of The Pas, Manitoba.

Disclosure statement

No potential conflict of interest was reported by the authors.

Funding

This work was supported by the Canada Excellence Research Chair at the Global Institute for Water Security, University of Saskatchewan and GIS Library Services, The Spatial Initiative, University of Saskatchewan.

References

Adams, P. N., R. L. Slingerland, and N. D. Smith. 2004. "Variations in Natural Levee Morphology in Anastomosed Channel Flood Plain Complexes." *Geomorphology* 61 (1–2): 127–142. doi:10.1016/j.geomorph.2003.10.005.

As-Syakur, A. R., I. S. Adnyana, I. W. Arthana, and I. W. Nuarsa. 2012. "Enhanced Built-Up and Bareness Index (EBBI) for Mapping Built-Up and Bare Land in an Urban Area." *Remote Sensing* 4 (12): 2957–2970. doi:10.3390/rs4102957.

Baschuk, M., M. Ervin, W. Clark, L. Armstrong, D. Wrubleski, and G. Goldsborough. 2012. "Using Satellite Imagery to Assess Macrophyte Response to Water-level Manipulations in the Saskatchewan River Delta, Manitoba." *Wetlands* 32 (6): 1091–1102. doi:10.1007/s13157-012-0339-z.

Baschuk, M., N. Koper, D. Wrubleski, and G. Goldsborough. 2012. "Effects of Water Depth, Cover and Food Resources on Habitat Use of Marsh Birds and Waterfowl in Boreal Wetlands of Manitoba, Canada." *Waterbirds* 35 (1): 44–55. doi:10.1675/063.035.0105.

Bayley, P. B. 1995. "Understanding Large River: Floodplain Ecosystems." *BioScience* 45 (3): 153–158. doi:10.2307/1312554.

Cowen, D. J., J. R. Jensen, P. J. Bresnahan, G. B. Ehler, D. Graves, X. Huang, and H. E. Mackey. 1995. "The Design and Implementation of an Integrated Geographic Information System for Environmental Applications." *Photogrammetric Engineering and Remote Sensing* 61 (11): 1393–1404.

Dangermond, J. 2013. "Understanding Our World with Landsat Data and ArcGIS." *ArcNews*, 35 (2): 1–3. http://www.esri.com/arcnews.

DUC. (2011). Summerberry Marsh *A Ducks Unlimited Canada Research Report* (A Ducks Unlimited Canada ed., pp. 18). The Pas: Institute for Wetland and Waterfowl Research, Ducks Unlimited Canada.

Fantin-Cruz, I., O. Pedrollo, N. M. R. Castro, P. Girard, P. Zeilhofer, and S. K. Hamilton. 2011. "Historical Reconstruction of Floodplain Inundation in the Pantanal (Brazil) Using Neural Networks." *Journal of Hydrology* 399 (3–4): 376–384. doi:10.1016/j.jhydrol.2011.01.014.

Feyisa, G. L., H. Meilby, R. Fensholt, and S. R. Proud. 2014. "Automated Water Extraction Index: A New Technique for Surface Water Mapping Using Landsat Imagery." *Remote Sensing of Environment* 140: 23–35. doi:10.1016/j.rse.2013.08.029.

Fournier, R. A., M. Grenier, A. Lavoie, and R. Hélie. 2007. "Towards a Strategy to Implement the Canadian Wetland Inventory Using Satellite Remote Sensing." *Canadian Journal of Remote Sensing* 33 (S1): S1–S16. doi:10.5589/m07-051.

Frohn, R. C., E. D'Amico, C. Lane, B. Autrey, J. Rhodus, and H. Liu. 2012. "Multi-temporal Sub-pixel Landsat ETM+ Classification of Isolated Wetlands in Cuyahoga County, Ohio, USA." *Wetlands* 32 (2): 289–299. doi:10.1007/s13157-011-0254-8.

Frohn, R. C., M. Reif, C. Lane, and B. Autrey. 2009. "Satellite Remote Sensing Of Isolated Wetlands Using Object-Oriented Classification of Landsat-7 Data." *Wetlands* 29 (3): 931–941. doi:10.1672/08-194.1.

Gao, B.-C. 1996. "NDWI—A Normalized Difference Water Index for Remote Sensing of Vegetation Liquid Water from Space." *Remote Sensing of Environment* 58 (3): 257–266. doi:10.1016/S0034-4257(96)00067-3.

Hess, L. L., and J. M. Melack. 2003. "Remote Sensing of Vegetation and Flooding on Magela Creek Floodplain (Northern Territory, Australia) with the SIR-C Synthetic Aperture Radar." *Hydrobiologia* 500 (1–3): 65–82. doi:10.1023/a:1024665017985.

Jain, S., A. Saraf, A. Goswami, and T. Ahmad. 2006. "Flood Inundation Mapping Using NOAA AVHRR Data." *Water Resources Management* 20 (6): 949–959. doi:10.1007/s11269-006-9016-4.

Jain, S., R. D. Singh, M. K. Jain, and A. K. Lohani. 2005. "Delineation of Flood-Prone Areas Using Remote Sensing Techniques." *Water Resources Management* 19 (4): 333–347. doi:10.1007/s11269-005-3281-5.

Jensen, J. 2007. *Remote Sensing of the Environment: An Earth Resource Perspective*. 2nd ed. Upper Saddle River, NJ: Pearson Prentice Hall.

Ji, L., L. Zhang, and B. Wylie. 2009. "Analysis of Dynamic Thresholds for the Normalized Difference Water Index." *Photogrammetric Engineering and Remote Sensing* 75 (11): 1307–1317. doi:10.14358/PERS.75.11.1307.

Kuenzer, C., M. Ottinger, M. Wegmann, H. Guo, C. Wang, J. Zhang, S. Dech, and M. Wikelski. 2014. "Earth Observation Satellite Sensors for Biodiversity Monitoring: Potentials and Bottlenecks." *International Journal of Remote Sensing* 35 (18): 6599–6647. doi:10.1080/01431161.2014.964349.

Lacaux, J. P., Y. M. Tourre, C. Vignolles, J. A. Ndione, and M. Lafaye. 2007. "Classification of Ponds from High-Spatial Resolution Remote Sensing: Application to Rift Valley Fever Epidemics in Senegal." *Remote Sensing of Environment* 106 (1): 66–74. doi:10.1016/j.rse.2006.07.012.

Lapp, S., D. Sauchyn, and B. Toth. 2009. "Constructing Scenarios of Future Climate and Water Supply for the SSRB: Use and Limitations for Vulnerability Assessment." *Prairie Forum* 34 (1): 153–180.

Lee, K. H., and E. N. Anagnostou. 2004. "A Combined Passive/Active Microwave Remote Sensing Approach for Surface Variable Retrieval Using Tropical Rainfall Measuring Mission Observations." *Remote Sensing of Environment* 92 (1): 112–125. doi:10.1016/j.rse.2004.05.003.

Li, X., W. Pichel, P. Clemente-Colón, V. Krasnopolsky, and J. Sapper. 2001. "Validation of Coastal Sea and Lake Surface Temperature Measurements Derived from NOAA/AVHRR Data." *International Journal of Remote Sensing* 22 (7): 1285–1303. doi:10.1080/01431160151144350.

Lira, J. 2006. "Segmentation and Morphology of Open Water Bodies from Multispectral Images." *International Journal of Remote Sensing* 27 (18): 4015–4038. doi:10.1080/01431160600702384.

McFeeters, S. K. 1996. "The Use of the Normalized Difference Water Index (NDWI) in the Delineation of Open Water Features." *International Journal of Remote Sensing* 17 (7): 1425–1432. doi:10.1080/01431169608948714.

Milewski, A., M. Sultan, S. M. Jayaprakash, R. Balekai, and R. Becker. 2009. "RESDEM, a Tool for Integrating Temporal Remote Sensing Data for Use in Hydrogeologic Investigations." *Computers & Geosciences* 35 (10): 2001–2010. doi:10.1016/j.cageo.2009.02.010.

Morozova, G. S., and N. D. Smith. 2000. "Holocene Avulsion Styles and Sedimentation Patterns of the Saskatchewan River, Cumberland Marshes, Canada." *Sedimentary Geology* 130 (1–2): 81–105. doi:10.1016/S0037-0738(99)00106-2.

Ouma, Y. O., and R. Tateishi. 2006. "A Water Index for Rapid Mapping of Shoreline Changes of Five East African Rift Valley Lakes: An Empirical Analysis Using Landsat TM and ETM+ Data." *International Journal of Remote Sensing* 27 (15): 3153–3181. doi:10.1080/01431160500309934.

Ozesmi, S., and M. Bauer. 2002. "Satellite Remote Sensing of Wetlands." *Wetlands Ecology and Management* 10 (5): 381–402. doi:10.1023/a:1020908432489.

PFRA. 1977. "Cumberland Lake Water Level Control Study." edited by P. F. R. A. Department of Agriculture. Saskatoon: Department of Northern Saskatchewan, Department of Agriculture, Prairie Farm Rehabilitation Administration.

Pomeroy, J., X. Fangn, C. Westbrook, A. Minke, X. Guo, and T. Brown. 2010. Prairie Hydrological Model Study Progress Report *Canadian Prairies* (Centre for Hydrology ed., Vol. Report # 7, pp. 113). Centre for Hydrology, University of Saskatchewan, Canada: Global Institute for Water Security.

Prowse, T. D., F. M. Conly, M. Church, and M. C. English. 2002. "A Review of Hydroecological Results of the Northern River Basins Study, Canada. Part 1. Peace and Slave Rivers." *River Research and Applications* 18 (5): 429–446. doi:10.1002/rra.681.

Reed, B., J. Brown, D. Vanderzee, T. Loveland, J. Merchant, and D. Ohlen. 1994. "Measuring Phenological Variability from Satellite Imagery." *Journal of Vegetation Science* 5 (5): 703–714. doi:10.2307/3235884.

Rokni, K., A. Ahmad, K. Solaimani, and S. Hazini. 2014. "A New Approach for Surface Water Change Detection: Integration of Pixel Level Image Fusion and Image Classification

Techniques." *International Journal of Applied Earth Observation and Geoinformation* 6: 4173–4189. doi:10.1016/j.jag.2014.08.014.
Sagintayev, Z., K. Chun, E. Hassanzadeh, K.-E. Lindenschmidt, T. Jardine, and H. Wheater. 2013. "Changes in Water Availability for the Saskatchewan River Delta." Paper presented at the 2013 Joint Scientific Congress of CMOS, CGU and CWRA, Saskatoon, May 26–30.
Sagintayev, Z., M. Sultan, S. D. Khan, S. A. Khan, K. Mahmood, E. Yan, A. Milewski, and P. Marsala. 2012. "A Remote Sensing Contribution to Hydrologic Modelling in Arid and Inaccessible Watersheds, Pishin Lora Basin, Pakistan." *Hydrological Processes* 26 (1): 85–99. doi:10.1002/hyp.8114.
Schindler, D., and W. Donahue. 2006. "An Impending Water Crisis in Canada's Western Prairie Provinces." *Proceedings of the National Academy of Sciences of the United States of America* 103 (19): 7210–7216. doi:10.1073/pnas.0601568103.
Shepherd, A., K. Gill, and S. Rood. 2010. "Climate Change and Future Flows of Rocky Mountain Rivers: Converging Forecasts from Empirical Trend Projection and Down-Scaled Global Circulation Modelling." *Hydrological Processes* 24 (26): 3864–3877. doi:10.1002/hyp.7818.
Smith, N., and M. Pérez-Arlucea. 2008. "Natural Levee Deposition during the 2005 Flood of the Saskatchewan River." *Geomorphology* 101 (4): 583–594. doi:10.1016/j.geomorph.2008.02.009.
Smith, N., M. Pérez-Arlucea, D. Edmonds, and R. Slingerland. 2009. "Elevation Adjustments of Paired Natural Levees during Flooding of the Saskatchewan River." *Earth Surface Processes and Landforms* 34 (8): 1060–1068. doi:10.1002/esp.1792.
SRBPartners. 2008. *Saskatchewan River Delta Symposium: Past, Present and Future, April* 1–3, *2008, Saskatoon, Saskatchewan: Proceedings*: Partners for the Saskatchewan River Basin.
St. Jacques, J., D. Sauchyn, and Y. Zhao. 2010. "Northern Rocky Mountain Streamflow Records: Global Warming Trends, Human Impacts or Natural Variability?" *Geophysical Research Letters* 37 (6): L06407. doi:10.1029/2009GL042045.
Sultan, M., N. Sturchio, S. A. Sefry, A. Milewski, R. Becker, I. Nasr, and Z. Sagintayev. 2008. "Geochemical, Isotopic, and Remote Sensing Constraints on the Origin and Evolution of the Rub Al Khali Aquifer System, Arabian Peninsula." *Journal of Hydrology* 356 (1–2): 70–83. doi:10.1016/j.jhydrol.2008.04.001.
Townsend, G. H. 1975. "Impact of Bennett Dam on Peace-Athabasca Delta." *Journal of the Fisheries Research Board of Canada* 32 (1): 171–176.
Töyrä, J., and A. Pietroniro. 2005. "Towards Operational Monitoring of a Northern Wetland Using Geomatics-Based Techniques." *Remote Sensing of Environment* 97 (2): 174–191. doi:10.1016/j.rse.2005.03.012.
van de Wolfshaar, K. E., H. Middelkoop, E. Addink, H. V. Winter, and L. A. J. Nagelkerke. 2011. "Linking Flow Regime, Floodplain Lake Connectivity and Fish Catch in a Large River-Floodplain System, the Volga–Akhtuba Floodplain (Russian Federation)." *Ecosystems* 14 (6): 920–934. doi:10.1007/s10021-011-9457-3.
Wagner, W., A. Luckman, J. Vietmeier, K. Tansey, H. Balzter, C. Schmullius, and J. J. Yu. 2003. "Large-Scale Mapping of Boreal Forest in SIBERIA Using ERS Tandem Coherence and JERS Backscatter Data." *Remote Sensing of Environment* 85 (2): 125–144. doi:10.1016/S0034-4257(02)00198-0.
Ward, D. P., S. K. Hamilton, T. D. Jardine, N. E. Pettit, E. K. Tews, J. M. Olley, and S. E. Bunn. 2013. "Assessing the Seasonal Dynamics of Inundation, Turbidity, and Aquatic Vegetation in the Australian Wetdry Tropics Using Optical Remote Sensing." *Ecohydrology* 6 (2): 312–323. doi:10.1002/eco.1270.
Wilson, E. H., and S. A. Sader. 2002. "Detection of Forest Harvest Type Using Multiple Dates of Landsat TM Imagery." *Remote Sensing of Environment* 80 (3): 385–396. doi:10.1016/S0034-4257(01)00318-2.
Winemiller, K. O. 2004. "Floodplain River Food Webs: Generalizations and Implications for Fisheries Management." Paper presented at the Second International Symposium on the Management of Large Rivers for Fisheries, Bangkok, Thailand. http://aquaticecology.tamu.edu/publications/
Xu, H. 2006. "Modification of Normalised Difference Water Index (NDWI) to Enhance Open Water Features in Remotely Sensed Imagery." *International Journal of Remote Sensing* 27 (14): 3025–3033. doi:10.1080/01431160600589179.